Electronic Supplementary Information

Organic Solar Cells Based on Small Molecule Donor and Polymer Acceptor Operating at 150 °C

Junhui Miao,[ab] Bin Meng,*[a] Zicheng Ding,[a] Jun Liu*[ab] and Lixiang Wang[ab]

[a]State Key Laboratory of Polymer Physics and Chemistry, Changchun Institute of Applied Chemistry, Chinese Academy of Sciences, Changchun 130022, P. R. China

[b]University of Science and Technology of China, School of Applied Chemistry and Engineering, Hefei 230026, P. R. China

*E-mail: mengbin@ciac.ac.cn (B.M.)

*E-mail: liujun@ciac.ac.cn (J.L.)

1. Experimental details

General. ^{1}H NMR and ^{13}C NMR spectra were measured with a Bruker AV-400 MHz NMR spectrometer at room temperature. Mass spectra were performed on a Bruker Daltonics Flex matrix-assisted laser desorption ionization time of flight mass spectrometer (MALDI-TOF-MS). Elemental analysis was recorded on a VarioEL elemental analyzer. The thermogravimetric analysis (TGA) was performed on a Perkin-Elmer 7 instrument at a heating rate of 10 ^{o}C min^{-1} under purified nitrogen gas (N_2) flow. The decomposition temperature (T_d) corresponded to 5% loss of weight. Differential scanning calorimetry (DSC) was performed with a TA DSC Q2000 instrument under purified nitrogen gas (N_2) flow at the heating and cooling rates of 10 ^{o}C min^{-1} in two heating/cooling cycles. The BD3T:PBN-14 (2.5:1, w/w) and BD3T:PBN-15 (2.5:1, w/w) blends for DSC characterization were prepared by drying their chlorobenzene (CB) solutions on the clean glass substrates and collecting the solids from the glass substrates. 2D grazing incidence wideangle X-ray scattering (2D-GIWAXS) were measured at the BL1W1A beamline at Beijing Synchrotron Radiation Facility (BSRF). Samples of pure materials or blends were prepared on silicon substrates. UV-vis absorption spectra (in CB solution and as thin films) were obtained with a Shimadzu UV-3600 spectrometer. Cyclic voltammogram (CV) measurements were performed on a CHI660a electrochemical workstation using glassy carbon as the working electrode, Pt wire as the counter electrode, and a standard calomel reference electrode in a 0.1 mol L^{-1} tetrabutylammonium hexafluorophosphate (Bu_4NPF_6) acetonitrile solution. The materials were casted on

the working electrode for measurements and ferrocene as an internal reference at a scan rate of 100 mV s^{-1}. The highest occupied molecular orbital (HOMO) and the lowest unoccupied molecular orbital (LUMO) energy levels of the materials were estimated by the equations: $E_{HOMO/LUMO} = -(4.80 + E_{onset}^{ox}/E_{onset}^{red})$ eV. The AFM images were recorded using a SPA300HV (Seiko Instruments, Inc., Japan) in tapping mode. Photoluminescence (PL) spectra were measured with a Horiba Jobin-Yvon FL3C-111 fluorescence spectrophotometer. The pure and blend film samples were fabricated by spin-coating the CB solutions onto quartz substrates with the exciting wavelength of 560 nm. The thickness of films was measured with a Dektak 6M Stylus Profilometer. Polarized optical microscopy was performed using Carl Zeiss Microlmaging GmbH Axio Imager A2m.

Materials and reagents. All chemicals and reagents were purchased from commercial sources and used without further purification unless otherwise mentioned. Toluene, tetrahydrofuran and chloroform were dried using sodium or calcium hydroxide before use. PBN-14 and PBN-15 were synthesized in our laboratory. 5''-bromo-3',3''-dioctyl-[2,2':5',2''-terthiophene]-5-carbaldehyde was prepared according to the reported method.

2. Syntheses and characterizations

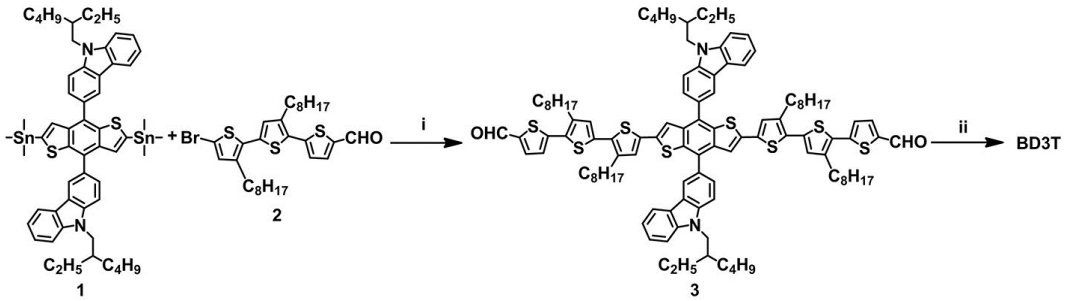

Figure S1. Synthetic route of BD3T. Reagents and conditions: (i) tetrakis(triphenylphosphine)palladium, toluene, 110 ^{o}C; (ii) 3-ethylrhodanine, chloroform, piperidine, 65 ^{o}C.

Monomer synthesis

5",5""-(4,8-bis(9-(2-ethylhexyl)-9*H*-carbazol-3-yl)benzo[1,2-b:4,5-b']dithiophene-2,6-diyl)bis(3',3"-dioctyl-[2,2':5',2"-terthiophene]-5-carbaldehyde) (**3**). In a 250 mL two-neck round bottom flask, 3,3'-(2,6-bis(trimethylstannyl)benzo[1,2-b:4,5-b']dithiophene-4,8-diyl)bis(9-(2-ethylhexyl)-9*H*-carbazole) (**1**) (0.50 g, 0.47 mmol), 5"-bromo-3',3"-dioctyl-[2,2':5',2"-terthiophene]-5-carbaldehyde (**2**) (0.62 g, 1.07 mmol) and Pd $(PPh_3)_4$ (0.14 g, 0.12 mmol) were dissolved in toluene (45 mL) under argon atmosphere. Then, the solution was stirred at 110 ^{o}C for 16 h. Subsequently, the solvent was removed and the crude product was purified by silica gel chromatography with 1:3 (v/v) petroleum ether–chloroform to give **3** (0.81 g, yielded 64%) as a red solid. ^{1}H NMR (400 MHz, $CDCl_3$): δ (ppm) 9.86 (s, 2H), 8.48 (s, 2H), 8.18 (d, J = 7.7 Hz, 2H), 7.84 (d, J = 10.0 Hz, 2H), 7.67 (d, J = 4.0 Hz, 2H), 7.63 (d, J = 8.4 Hz, 2H), 7.56-7.48 (m, 4H), 7.44 (s, 2H), 7.29 (t, J = 7.6 Hz, 2H), 7.18 (d, J = 4.0 Hz, 2H), 7.04 (s, 2H), 6.94 (s, 2H), 4.35-4.25 (m, 4H), 2.78-2.74 (m, 4H), 2.72-2.68 (m, 4H), 2.25-2.18 (m, 2H), 1.67-1.57 (m, 8H), 1.52-1.18 (m, 56H), 1.05-1.01 (m, 6H), 0.95-0.91 (m, 6H), 0.88-0.82 (m, 12H). ^{13}C NMR(100 MHz, $CDCl_3$): δ (ppm) 182.53, 146.13, 142.54, 142.12, 141.55, 141.10, 140.80, 138.71, 137.57, 137.19, 136.82, 136.07, 135.86, 130.56, 130.04, 129.34, 128.96, 128.20, 126.93, 126.06, 125.86, 125.80, 123.33, 122.82, 121.20, 120.61, 119.21, 119.11, 109.47, 109,27, 47.73, 39.64, 31.87,

31.84, 31.11, 30.32, 30.21, 29.74, 29.61, 29.57, 29.55, 29.41, 29.38, 29.35, 29.24, 29.21, 28.88, 24.56, 23.17, 22.66, 22.64, 14.12, 14.09, 11.01. MS (MALDI-TOF): Calculated for $C_{108}H_{128}N_2O_2S_8$ [M^+], 1740.8; found, 1740.8. Elemental analyses calculated (%) for $C_{108}H_{128}N_2O_2S_8$: C, 74.43; H, 7.40; N, 1.61. Found: C, 74.38; H, 7.37; N, 1.58.

BD3T: Compound (**3**) (0.40 g, 0.23 mmol) and 3-ethylrhodanine (0.37 g, 2.30 mmol) were dissolved in anhydrous $CHCl_3$ (80 mL), and then five drops of piperidine were added to the mixture. After refluxed for 16 h, the mixture was poured into water and then extracted with $CHCl_3$, the organic layer was dried over anhydrous Na_2SO_4. After removal of solvent, the crude product was purified by silica gel chromatography with 1:4 (v/v) petroleum ether–chloroform to give **BD3T** (0.40 g, yielded 85%) as a brown solid. ^{1}H NMR (400 MHz, $CDCl_3$): δ (ppm) 8.48 (s, 2H), 8.18 (d, J = 7.7 Hz, 2H), 7.83 (d, J = 7.6 Hz, 2H), 7.81 (s, 2H), 7.61 (d, J = 6.8 Hz, 2H), 7.54 (t, J = 7.6 Hz, 2H), 7.49 (d, J = 8.2 Hz, 2H), 7.43 (s, 2H), 7.31-7.27 (m, 4H), 7.15 (d, J = 3.2 Hz, 2H), 7.02 (s, 2H), 6.92 (s, 2H), 4.31-4.22 (m, 4H), 4.17 (m, 4H), 2.74 (m, 4H), 2.69 (m, 4H), 2.25-2.15 (m, 2H), 1.67-1.58 (m, 8H), 1.55-1.22 (m, 62H), 1.04-1.01 (m, 6H), 0.95-0.92 (m, 6H), 0.87-0.82 (m, 12H). ^{13}C NMR(100 MHz, $CDCl_3$) δ (ppm) 191.94, 167.27, 144.37, 141.94, 141.54, 140.97, 140.79, 138.68, 137.55, 137.16, 136.98, 135.78, 135.76, 134.64, 130.49, 130.16, 129.58, 129.51, 128.95, 128.18, 126.93, 126.49, 126.04, 125.03, 125.00, 123.31, 122.84, 121.21, 120.63, 120.21, 119.18, 119.09, 109.44, 109.25, 47.72, 39.92, 39.63, 31.86, 31.11, 30.28, 29.79, 29.70, 29.64, 29.61, 29.56, 29.44, 29.37, 29.27, 29.22, 28.88, 24.56, 23.17, 22.67, 22.64, 14.11,

14.09, 12.27, 11.02, -0.01. MS (MALDI-TOF): Calculated for $C_{118}H_{138}N_4O_2S_{12}$ [M^+], 2026.8; found, 2026.8. Elemental analyses calculated (%) for $C_{118}H_{138}N_4O_2S_{12}$: C, 69.84; H, 6.85; N, 2.76. Found: C, 69.78; H, 6.82; N, 2.74.

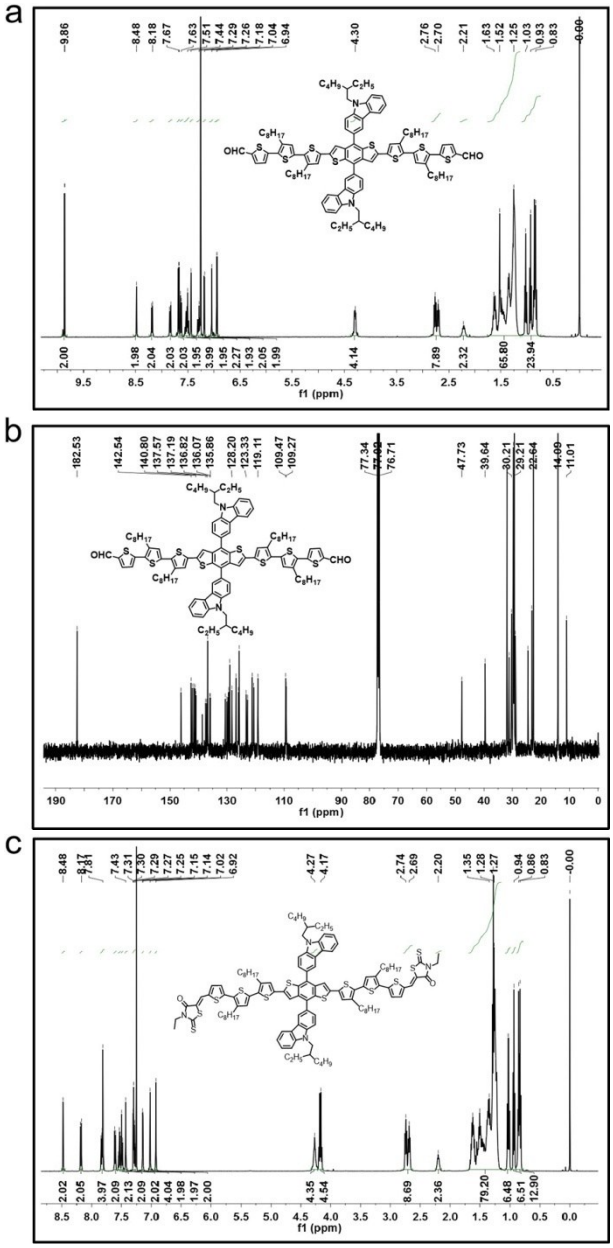

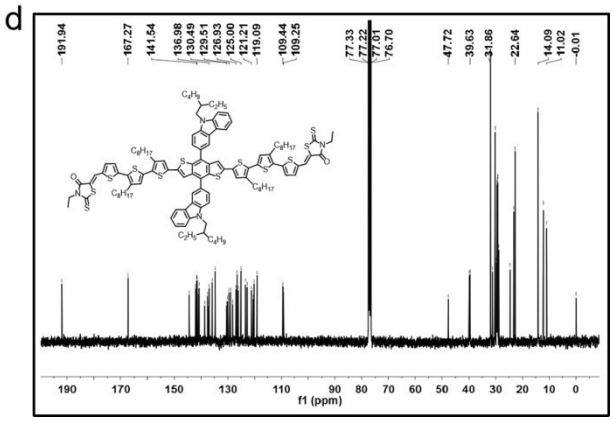

Figure S2. a, c) ^{1}H NMR, b, d) ^{13}C NMR of **3** and **BD3T**.

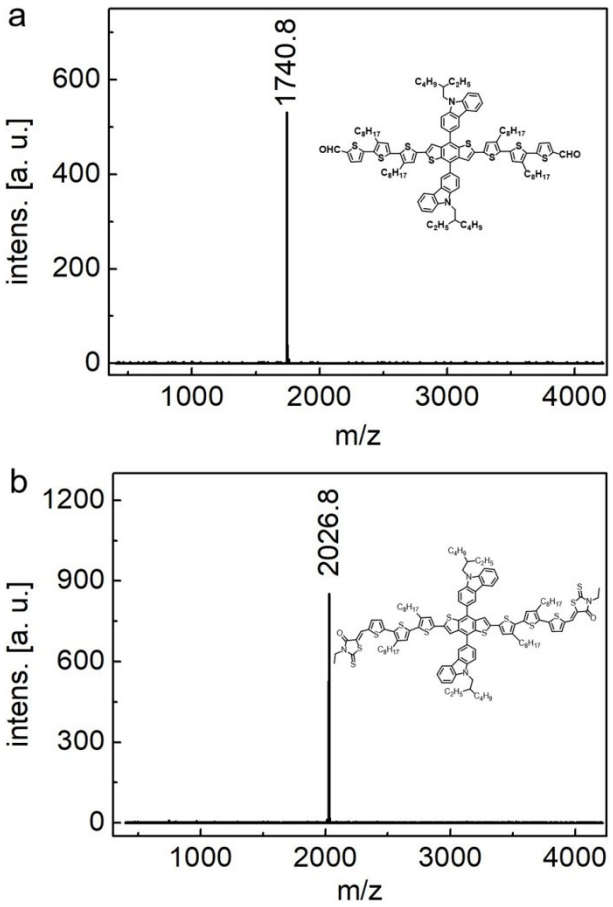

Figure S3. MALDI-TOF MS results of a) **3** and b) **BD3T**.

3. Thermal properties

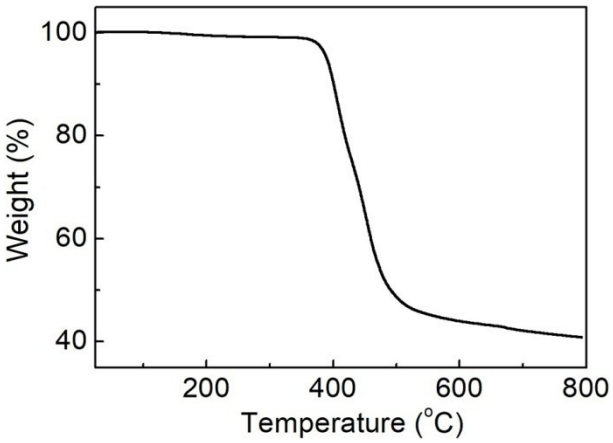

Figure S4. TGA curve of **BD3T** under N_2 atmosphere at a scan rate of 10 ^{o}C min^{-1}.

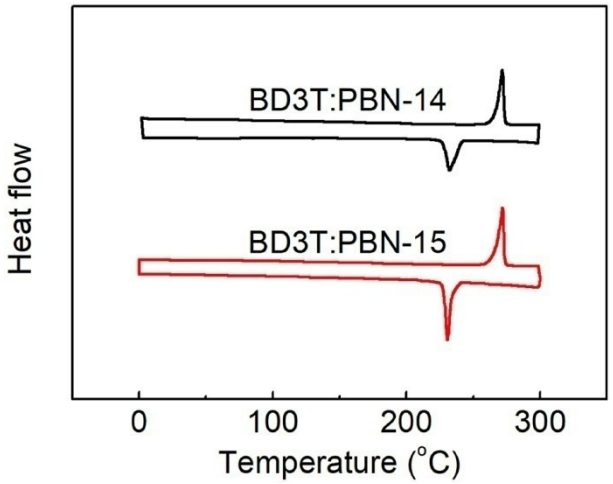

Figure S5. DSC second heating and cooling cycles of BD3T:PBN-14 blend (2.5:1, w/w) and BD3T:PBN-15 blend (2.5:1, w/w) under N_2 atmosphere at a scan rate of 10 ^{o}C min^{-1}.

Table S1. The thermal behavior parameters of the pure BD3T, BD3T:PBN-14 blend and BD3T:PBN-15 blend.

	T_m (°C)	ΔH_m (J/g)	T_c (°C)	ΔH_c (J/g)
BD3T	273.4	54.9	243.4	52.6
BD3T:PBN-14	271.6	35.5	232.3	32.3
BD3T:PBN-15	271.9	35.3	230.7	32.2

4. UV-vis absorption spectra and stacking properties of the materials

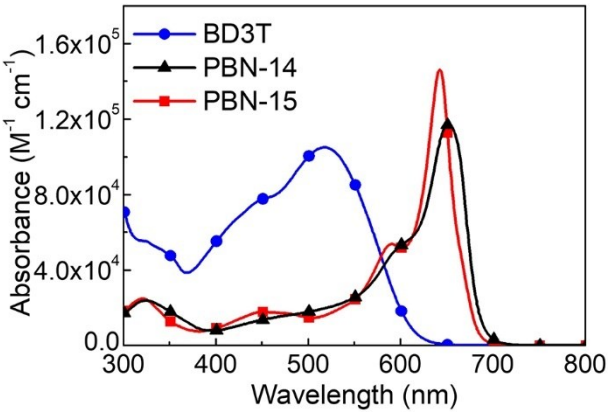

Figure S6. UV-vis absorption spectra of BD3T, PBN-14 and PBN-15 in CB solution.

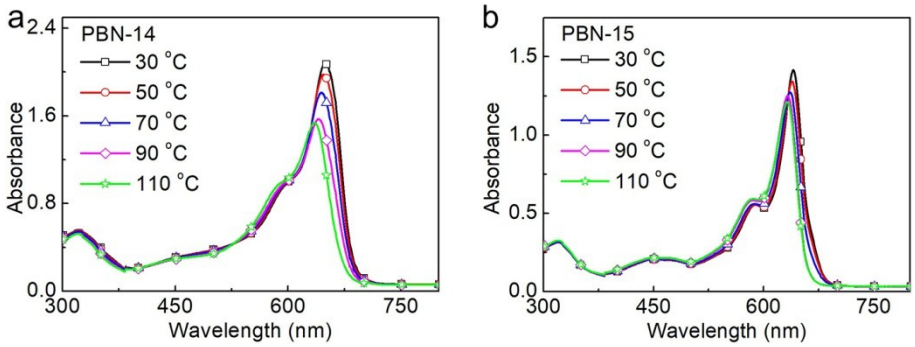

Figure S7. Temperature-dependent UV/vis absorption spectra of PBN-14 and PBN-15 in CB solution.

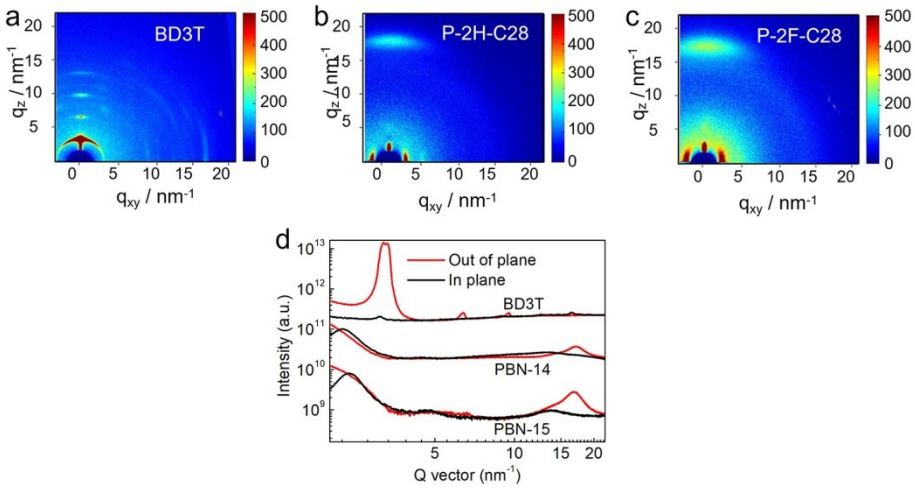

Figure S8. 2D-GIWAXS patterns of pristine (a) BD3T, (b) PBN-14, (c) PBN-15 and (d) 1D profiles of the three pristine films.

Table S2. 2D-GIWAXS characterization data of the pristine BD3T, PBN-14 and PBN-15 films and the BD3T:PBN-14 and BD3T:PBN-15 blend films.

Films	Directions	100				010			
		Location [Å^{-1}]	d-spacing [Å]	FWHM [Å^{-1}]	CCL [Å]	Location [Å^{-1}]	d-spacing [Å]	FWHM [Å^{-1}]	CCL [Å]
BD3T	Out-of- plane	0.32	19.63	0.0265	213				
	In-plane					1.64	3.83	0.0659	86
PBN-14	Out-of- plane					1.71	3.67	0.290	19
	In-plane	0.22	28.56	0.0640	88				
PBN-15	Out-of- plane					1.67	3.76	0.170	33
	In-plane	0.24	26.18	0.0581	97				
BD3T:PBN-14	Out-of- plane	0.32	19.57	0.0420	135	1.65	3.80	0.072	78
	In-plane	0.31	20.40	0.0274	206				
BD3T:PBN-15	Out-of- plane	0.32	19.82	0.0466	121	1.65	3.80	0.108	52
	In-plane	0.31	20.47	0.0295	192				

5. OSC devices fabrication and measurement

The OSC devices were fabricated with the structure of ITO/ZnO/active layer/MoO_3/Al. ITO glass substrates were cleaned in an ultrasonic bath with deionized water, acetone, and isopropyl alcohol, and then dried at 125 ^{o}C for 30 min. After treated with ultraviolet–ozone for 15 min, ZnO layers (ca. 30 nm) was spin-coated at 5000 rpm onto the cleaned ITO glasses from ZnO precursor solution, and then baked at 200 ^{o}C for 60 min in air. The ZnO precursor was synthesized by dissolving zinc acetate dehydrate (200 mg) and ethanolamine (65 mg) in 2 mL 2-methoxyethanol under vigorous stirring for 10 h in air. All of the substrates were

placed into an nitrogen-filled glove box. Subsequently, BD3T:PBN-14 or BD3T:PBN-15 (2.5:1 weight ratio) based blends were dissolved in CB (0.3% diphenyl ether (DBE) as the additive) with a concentration of 10.5 mg/mL. The solutions were stirred at 110 °C for 3 h, and then spin-coated at 1800 rpm for 60 s onto the substrates to obtain the active layers (ca. 100 nm). And the active layers were thermal annealed at 180 °C for 10 min. Then, the device fabrication was completed by thermally evaporating MoO_3 (15 nm) and aluminum (100 nm) under vacuum at a pressure of 2×10^{-4} Pa. The active area of the devices, defined by a shadow mask, was 2 mm^2. The current density (*J–V*) curves of the OSC devices were measured using a computer-controlled Keithley 2400 sourcemeter under 100 mW cm^{-2} AM 1.5G simulated solar light illumination. An XES-40S2-CE class solar simulator (Japan, SAN-EI Electric Co., Ltd) was used to provide the AM 1.5G simulated solar light illumination. The EQE spectra were measured using a Solar Cell Spectral Response Measurement System QE-R3011 (Enlitech Co., Ltd). The light intensity at each wavelength was calibrated using a calibrated monosilicon diode.

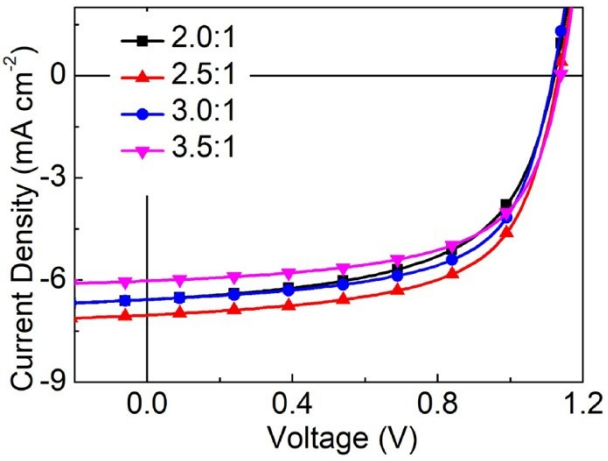

Figure S9. *J–V* plots of the OSCs based on BD3T:PBN-14 blend films with thermal annealing at 180 °C with different D:A ratios.

Table S3. Photovoltaic parameters of the solar cells based on BD3T:PBN-14 blend films with thermal annealing at 180 °C with different D:A ratios under illumination of AM 1.5 G, 100 mW cm^{-2}.

D:A ratio	V_{OC} (V)	J_{SC} (mA/cm^2)	FF	PCE (%)
2.0:1	1.12	6.58	0.58	4.30
2.5:1	1.13	7.03	0.62	4.96
3.0:1	1.12	6.58	0.62	4.58
3.5:1	1.14	6.03	0.63	4.24

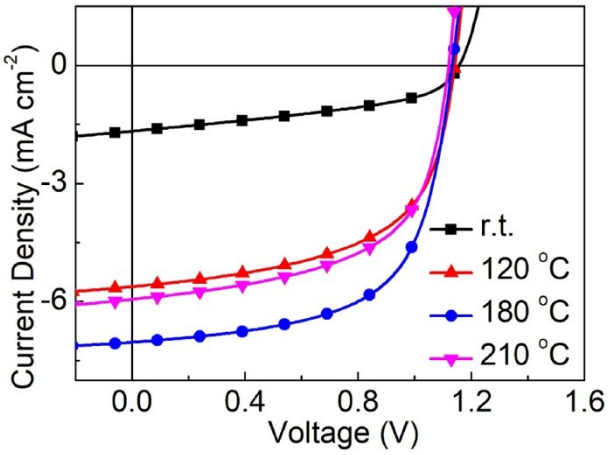

Figure S10. *J–V* plots of the OSCs based on BD3T:PBN-14 blend films (2.5:1, w/w) with different annealing temperature.

Table S4. Photovoltaic parameters of the solar cells based on BD3T:PBN-14 blend films (2.5:1, w/w) with different annealing temperature under illumination of AM 1.5 G, 100 mW cm^{-2}.

Annealing temperature (°C)	V_{OC} (V)	J_{SC} (mA/cm^2)	FF	PCE (%)
r.t.	1.16	1.17	0.44	0.86
120	1.14	5.62	0.58	3.72
180	1.13	7.03	0.62	4.96
210	1.12	5.94	0.59	3.92

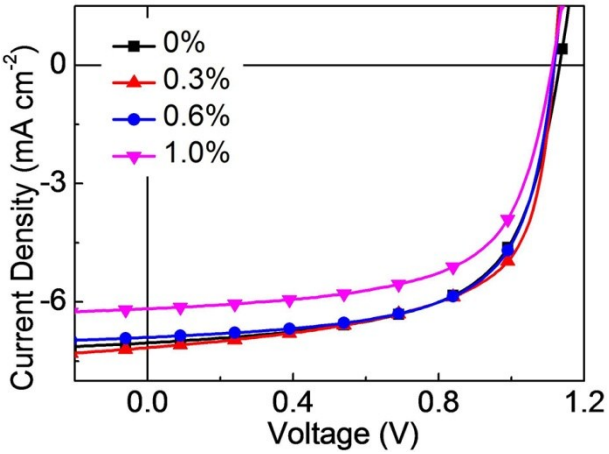

Figure S11. *J–V* plots of the OSCs based on BD3T:PBN-14 blend films (2.5:1, w/w) with annealing temperature at 180 °C with different DBE contents.

Table S5. Photovoltaic parameters of the solar cells based on BD3T:PBN-14 blend films (2.5:1, w/w) with annealing temperature at 180 °C with different DBE contents under illumination of AM 1.5 G, 100 mW cm^{-2}.

DBE content (%)	V_{OC} (V)	J_{SC} (mA/cm^2)	FF	PCE (%)
0	1.13	7.03	0.62	4.96
0.3	1.12	7.16	0.63	5.06
0.6	1.12	6.90	0.65	4.99
1.0	1.11	6.17	0.63	4.33

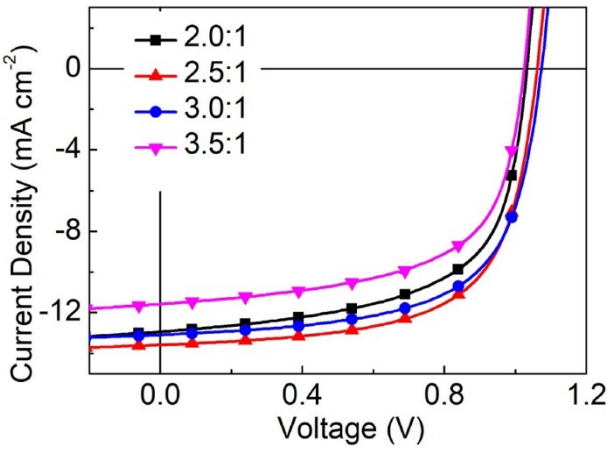

Figure S12. *J–V* plots of the OSCs based on BD3T:PBN-15 blend films with thermal annealing at 180 °C with different D:A ratios.

Table S6. Photovoltaic parameters of the solar cells based on BD3T:PBN-15 blend films with thermal annealing at 180 °C with different D:A ratios under illumination of AM 1.5 G, 100 mW cm^{-2}.

D:A ratio	V_{OC} (V)	J_{SC} (mA/cm^2)	FF	PCE (%)
2.0:1	1.03	12.94	0.62	8.29
2.5:1	1.04	13.57	0.65	9.13
3.0:1	1.04	13.07	0.64	8.69
3.5:1	1.05	11.60	0.62	7.49

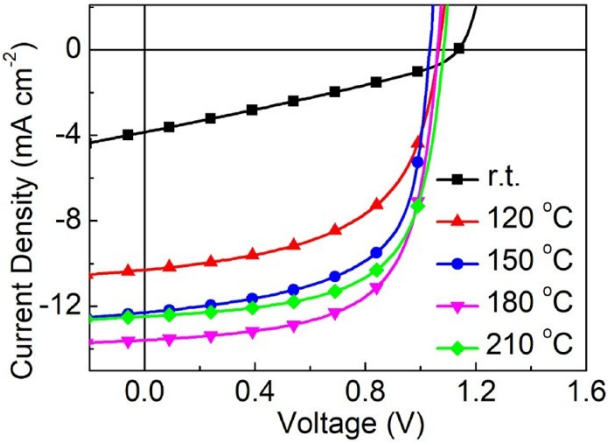

Figure S13. *J–V* plots of the OSCs based on BD3T:PBN-15 blend films (2.5:1, w/w) with different annealing temperature.

Table S7. Photovoltaic parameters of the solar cells based on BD3T:PBN-15 blend films (2.5:1, w/w) with different annealing temperature under illumination of AM 1.5 G, 100 mW cm^{-2}.

Annealing temperature (°C)	V_{OC} (V)	J_{SC} (mA/cm^2)	FF	PCE (%)
r.t.	1.14	3.85	0.31	1.37
120	1.07	10.30	0.56	6.14
150	1.04	12.31	0.63	8.07
180	1.04	13.57	0.65	9.13
210	1.03	12.45	0.64	8.18

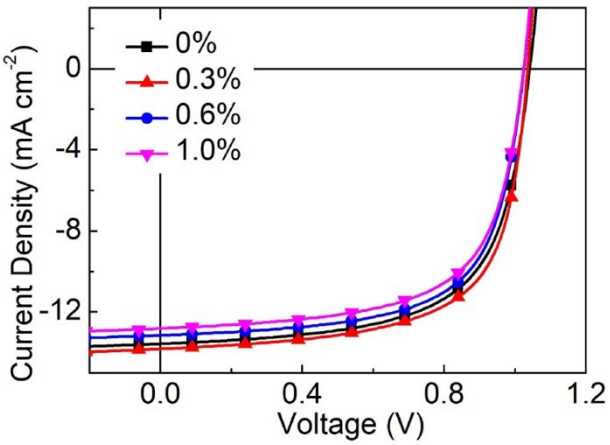

Figure S14. *J–V* plots of the OSCs based on BD3T:PBN-15 blend films (2.5:1, w/w) with annealing temperature at 180 °C with different DBE contents.

Table S8. Photovoltaic parameters of the solar cells based on BD3T:PBN-15 blend films (2.5:1, w/w) with annealing temperature at 180 °C with different DBE contents under illumination of AM 1.5 G, 100 mW cm^{-2}.

DBE content (%)	V_{OC} (V)	J_{SC} (mA/cm^2)	FF	PCE (%)
0	1.04	13.57	0.65	9.13
0.3	1.04	13.82	0.66	9.51
0.6	1.03	13.15	0.66	8.84
1.0	1.02	12.82	0.65	8.47

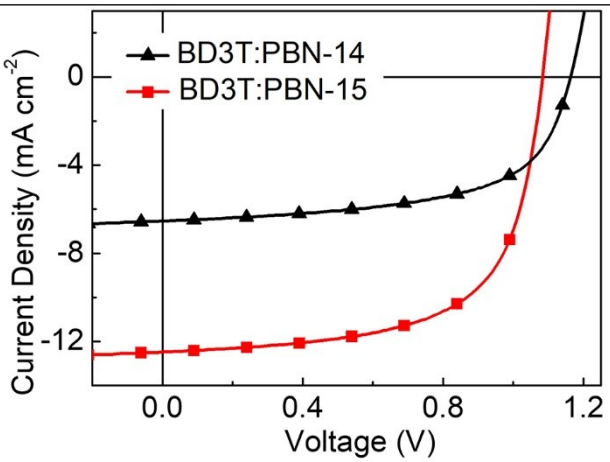

Figure S15. *J–V* plots of the OSCs based on BD3T:PBN-14 and BD3T:PBN-15 blend films with the active area of 8 mm^2 under illumination of AM 1.5 G, 100 mW cm^{-2}.

Table S9. Photovoltaic parameters of the solar cells based on BD3T:PBN-14 and BD3T:PBN-15 blend films with the active area of 8 mm^2 under illumination of AM 1.5 G, 100 mW cm^{-2}.

Active layer	V_{OC} (V)	J_{SC} (mA/cm^2)	FF	PCE (%) [a]
BD3T:PBN-14	1.16 (1.16 ± 0.01)	6.53 (6.42 ± 0.12)	0.60 (0.60 ± 0.01)	4.55 (4.46 ± 0.07)
BD3T:PBN-15	1.08 (1.08 ± 0.01)	12.48 (12.33 ± 0.22)	0.64 (0.64 ± 0.01)	8.67 (8.49 ± 0.12)

[a] Devices were measured from 12 devices with best values (outside of parentheses) and statistical average values with error bars of standard deviation (in parentheses).

6. Hole/electron-only devices fabrication and hole/electron mobility measurement

The hole/electron mobilities were measured using the space charge limited current (SCLC) method. The hole-only device structure for the BD3T film is ITO/PEDOT:PSS/BD3T/MoO_3/Al and the electron-only devices structure for polymer acceptors are ITO/PEIE/PBN-14 or PBN-15/Ca/Al. The hole-only and electron-only device structures for the active layers are ITO/PEDOT:PSS/active layer/MoO_3/Al and ITO/PEIE/active layer/Ca/Al, respectively. The current-voltage curves in the range of 0–8 V were recorded using a computer-controlled Keithley 2400 source meter, and the results were fitted to a space-charge limited function:

$$J = \frac{9}{8}\varepsilon_r\varepsilon_0\mu\frac{V^2}{L^3}\exp\left(0.89\beta\frac{\sqrt{V}}{\sqrt{L}}\right)$$

where J is the current density, ε_0 is the permittivity of free space, ε_r is the relative permittivity of 3 for molecules, μ is the zero-field mobility, V is the potential across the device ($V = V_{applied} - V_{bias} - V_{series}$), L is the thickness of active layer, and β is the field-activation factor. The series and contact resistance (V_{series}) of the device (10–15

Ω) were measured using blank device of ITO/PEDOT:PSS/MoO_3/Al or ITO/PEIE/Ca/Al. The range of 0–5 V was used to extract the mobility values.

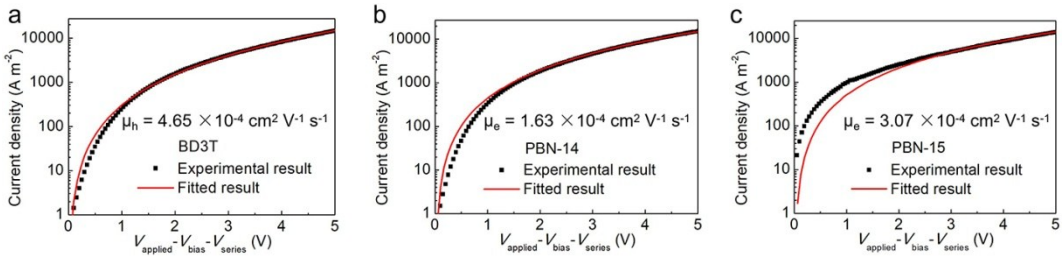

Figure S16. *J–V* curves and SCLC fittings of the hole-only device of a) BD3T film and electron-only devices of b) PBN-14 film and c) PBN-15 film.

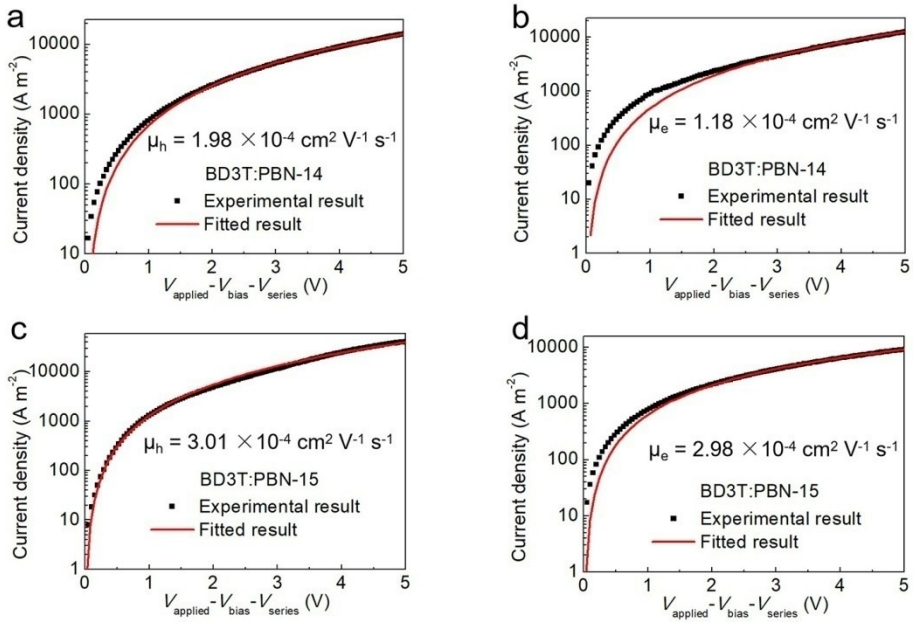

Figure S17. *J–V* curves and SCLC fittings a, c) the hole-only device and b, d) the electron-only device based on the BD3T:PBN-14 blend and the BD3T:PBN-15 blend, respectively.

7. The photoluminescence (PL) measurements

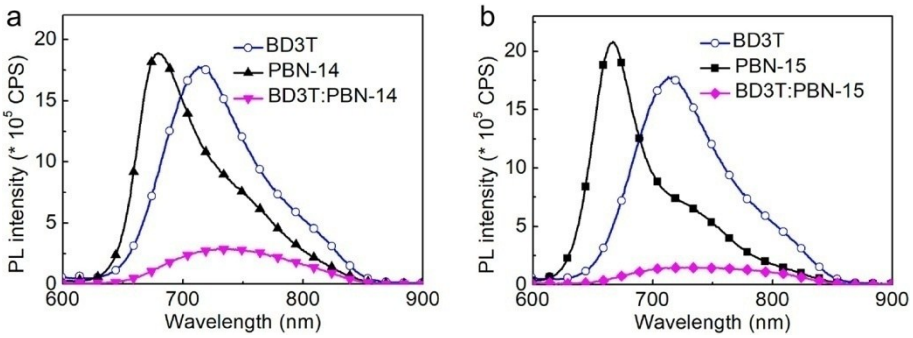

Figure S18. Photoluminescence spectra of a) pure BD3T, PBN-14 film and BD3T:PBN-14 blend film, and b) pure BD3T, PBN-15 film and BD3T:PBN-15 blend film.

8. Charge generation, collection and recombination behaviors

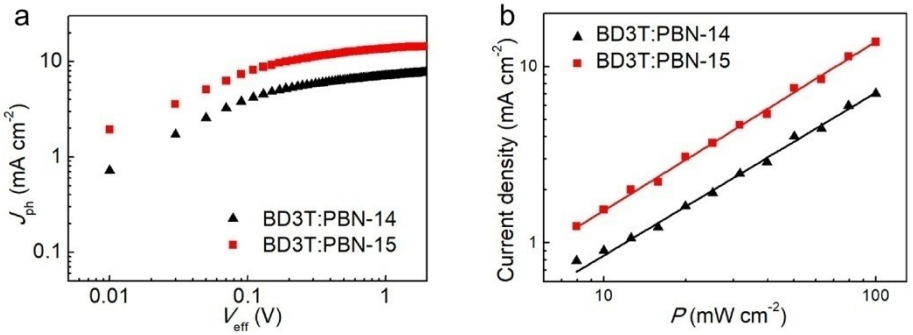

Figure S19. a) J_{ph} versus V_{eff} plots; b) dependence of J_{SC} on light intensity for OSCs based on BD3T:PBN-14 and BD3T:PBN-15.

9. The thermal stability OSC devices fabrication and test

The thermal stability OSC devices were fabricated with the structure of ITO/ZnO/active layer/PEDOT:PSS (2% FS-31)/Ag. The ITO/ZnO substrates were prepared by the aforementioned method. The optimal active layer solutions of BD3T:PBN-15 or PTB7-Th:EH-IDTBR were spin-coated onto the ITO/ZnO substrates, then the active layers were thermal annealed. PEDOT:PSS (2% FS-31) was the PEDOT:PSS solution with 2 vol% FS-31 and 2 vol% isopropanol, where FS-31 was used as the surfactant to enhance the wettability of PEDOT:PSS and

isopropanol was used as additive to increase the conductivity of PEDOT:PSS. The PEDOT:PSS (2% FS-31) was deposited on the active layers through spin coating at 5000 rpm for 40 s in air, and then annealed at 120 °C for 30 min in the glove box. Finally, the Ag electrodes were deposited on the top of the PEDOT:PSS at a pressure of 2×10^{-4} Pa to fabricated the thermal stability devices. For different test temperature of the devices, the devices were first heated to the specified temperature by the temperature-controlled heater plate, then the XES-40S2-CE class solar simulator was used to test the devices in the glove box. For the test of different thermal treatment of the devices, the devices were first thermal treatment at 150 °C for different time, then tested at room temperature. For the thermal stability test of the active layers, the active layers were first thermal treatment at 150 °C for different time, and then MoO_3 and Al were deposited onto the active layers to obtain the devices.

Table S10. Photovoltaic parameters of the OSC devices based on BD3T:PBN-15 blend with different test temperature under illumination of AM 1.5 G, 100 mW cm^{-2}.

Test temperature (°C)	V_{OC} (V)	J_{SC} (mA/cm²)	FF	PCE (%)[a]
25	1.01 ± 0.01	12.85 ± 0.16	0.62 ± 0.01	8.01 ± 0.20
50	1.01 ± 0.01	13.13 ± 0.34	0.61 ± 0.01	8.14 ± 0.18
80	1.00 ± 0.02	13.41 ± 0.27	0.60 ± 0.01	8.07 ± 0.21
120	0.99 ± 0.01	13.48 ± 0.19	0.60 ± 0.01	8.01 ± 0.20
150	0.98 ± 0.01	13.59 ± 0.36	0.59 ± 0.01	7.85 ± 0.23
160	0.97 ± 0.01	13.62 ± 0.33	0.57 ± 0.01	7.66 ± 0.25
180	0.94 ± 0.01	10.72 ± 0.28	0.57 ± 0.01	5.76 ± 0.24
210	0.77 ± 0.01	10.03 ± 0.60	0.56 ± 0.01	4.29 ± 0.36

[a] The PCE values were obtained from six individual devices.

Table S11. Photovoltaic parameters of the OSC devices based on PTB7-Th:EH-IDTBR blend with different test temperature under illumination of AM 1.5 G, 100 mW cm^{-2}.

Test temperature (°C)	V_{OC} (V)	J_{SC} (mA/cm^2)	FF	PCE (%)[a]
25	0.95 ± 0.01	16.28 ± 0.30	0.59 ± 0.01	9.05 ± 0.22
50	0.94 ± 0.01	16.16 ± 0.19	0.58 ± 0.01	8.81 ± 0.20
80	0.94 ± 0.01	16.17 ± 0.20	0.58 ± 0.01	8.83 ± 0.20
120	0.93 ± 0.01	16.62 ± 0.42	0.57 ± 0.01	8.81 ± 0.23
150	0.92 ± 0.01	16.65 ± 0.29	0.57 ± 0.01	8.73 ± 0.23
160	0.92 ± 0.01	16.76 ± 0.33	0.56 ± 0.01	8.63 ± 0.25
180	0.85 ± 0.01	11.62 ± 0.53	0.55 ± 0.01	5.45 ± 0.32
210	0.76 ± 0.01	10.01 ± 0.54	0.51 ± 0.01	3.86 ± 0.31

[a] The PCE values were obtained from six individual devices.

Table S12. Photovoltaic parameters of the OSC devices based on BD3T:PBN-15 blend with different thermal treatment time under illumination of AM 1.5 G, 100 mW cm^{-2}.

Annealing time (h)	V_{OC} (V)	J_{SC} (mA/cm^2)	FF	PCE (%)[a]
0	1.01 ± 0.01	12.85 ± 0.16	0.62 ± 0.01	8.01 ± 0.20
1	1.01 ± 0.01	12.68 ± 0.16	0.62 ± 0.01	7.90 ± 0.18
2	1.01 ± 0.01	12.66 ± 0.29	0.61 ± 0.01	7.80 ± 0.23
4	1.01 ± 0.01	12.37 ± 0.28	0.62 ± 0.01	7.64 ± 0.17
8	1.01 ± 0.01	12.37 ± 0.26	0.61 ± 0.01	7.52 ± 0.21
24	1.01 ± 0.01	12.18 ± 0.23	0.61 ± 0.01	7.41 ± 0.21
36	0.99 ± 0.01	12.38 ± 0.37	0.59 ± 0.01	7.18 ± 0.24
48	0.97 ± 0.01	11.85 ± 0.33	0.61 ± 0.01	6.97 ± 0.28
72	0.95 ± 0.01	11.80 ± 0.34	0.61 ± 0.01	6.76 ± 0.21

[a] The PCE values were obtained from six individual devices.

Table S13. Photovoltaic parameters of the OSC devices based on PTB7-Th:EH-IDTBR blend with different thermal treatment time under illumination of AM 1.5 G, 100 mW cm^{-2}.

Annealing time (h)	V_{OC} (V)	J_{SC} (mA/cm^2)	FF	PCE (%)[a]
0	0.95 ± 0.01	16.28 ± 0.30	0.59 ± 0.01	9.05 ± 0.22
1	0.93 ± 0.01	15.76 ± 0.49	0.56 ± 0.01	8.21 ± 0.22
2	0.93 ± 0.01	15.24 ± 0.54	0.55 ± 0.01	7.74 ± 0.23
4	0.92 ± 0.01	15.37 ± 0.41	0.54 ± 0.01	7.64 ± 0.26
8	0.90 ± 0.01	14.85 ± 0.28	0.53 ± 0.01	7.14 ± 0.20
24	0.90 ± 0.01	14.34 ± 0.71	0.54 ± 0.01	6.92 ± 0.24
36	0.90 ± 0.01	14.00 ± 0.41	0.53 ± 0.01	6.63 ± 0.21
48	0.89 ± 0.01	13.59 ± 0.47	0.51 ± 0.01	6.21 ± 0.24
72	0.89 ± 0.01	12.15 ± 0.70	0.52 ± 0.01	5.58 ± 0.28

[a] The PCE values were obtained from six individual devices.

10. The morphology change in the active layer after the thermal treatment

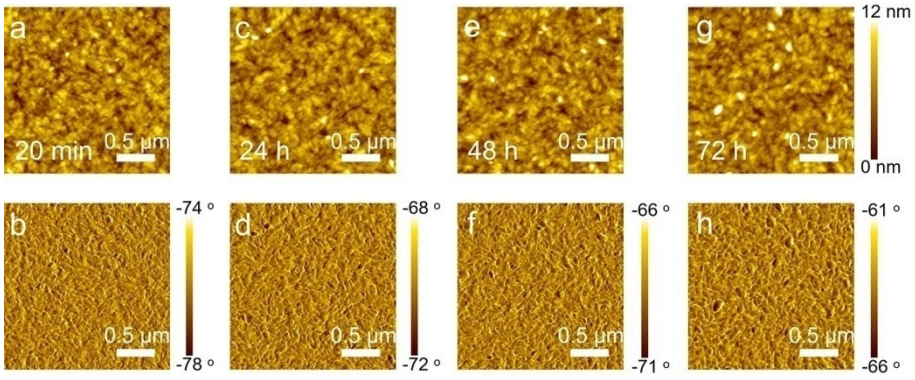

Figure S20. AFM (a, c, e and g) height images and (b, d, f and h) phase images of BD3T:PBN-15 blends with thermal treatment at 150 °C for different time.

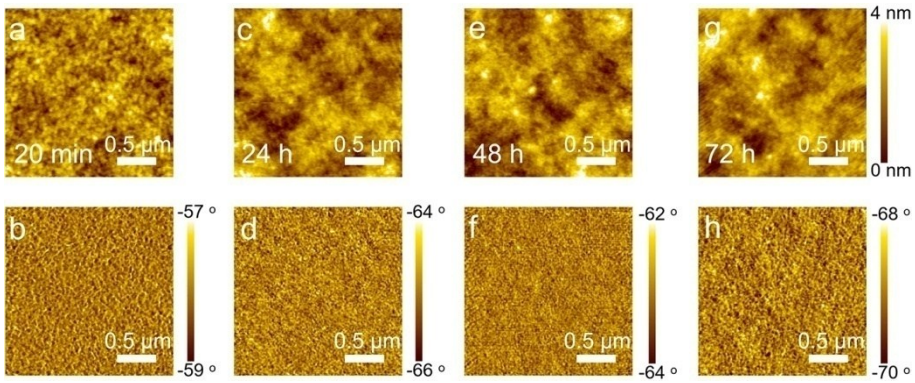

Figure S21. AFM (a, c, e and g) height images and (b, d, f and h) phase images of PTB7-Th:EH-IDTBR blends with thermal treatment at 150 ^{o}C for different time.